Surface water dynamics and rapid lake drainage in the Western Canadian Subarctic (1985–2020)

H. Z. Travers-Smith, T. C. Lantz, & R. H. Fraser

2021

Original citation:
Travers-Smith, H. Z., Lantz, T. C., & Fraser, R. H. (2021). Surface water dynamics and rapid lake drainage in the Western Canadian Subarctic (1985–2020). *Journal of Geophysical Research Biogeosciences*, *126*(12).
https://doi.org/10.1029/2021jg006445

JGR Biogeosciences

RESEARCH ARTICLE
10.1029/2021JG006445

Key Points:

- 43% of lakes showed a significant trend in surface area and the majority of these changes (65%) were non-linear in nature
- Thermokarst processes following wildfire have likely contributed to declines in lake area
- Soil texture and surficial geology also influenced the direction of change in lake area

Supporting Information:

Supporting Information may be found in the online version of this article.

Correspondence to:

H. Z. Travers-Smith,
hztraver@uvic.ca

Citation:

Travers-Smith, H. Z., Lantz, T. C., & Fraser, R. H. (2021). Surface water dynamics and rapid lake drainage in the western Canadian subarctic (1985–2020). *Journal of Geophysical Research: Biogeosciences*, *126*, e2021JG006445. https://doi.org/10.1029/2021JG006445

Received 13 MAY 2021
Accepted 3 DEC 2021

Author Contributions:

Conceptualization: T. C. Lantz
Formal analysis: H. Z. Travers-Smith
Funding acquisition: T. C. Lantz
Investigation: H. Z. Travers-Smith
Methodology: H. Z. Travers-Smith, R. H. Fraser
Project Administration: T. C. Lantz
Supervision: T. C. Lantz, R. H. Fraser
Visualization: H. Z. Travers-Smith
Writing – original draft: H. Z. Travers-Smith
Writing – review & editing: T. C. Lantz, R. H. Fraser

Surface Water Dynamics and Rapid Lake Drainage in the Western Canadian Subarctic (1985–2020)

H. Z. Travers-Smith[1], T. C. Lantz[1], and R. H. Fraser[2]

[1]School of Environmental Studies, University of Victoria, Victoria, BC, Canada, [2]Canada Centre for Mapping and Earth Observation, Natural Resources, Ottawa, ON, Canada

Abstract The area and distribution of surface water are shifting rapidly in many regions across the circumpolar Arctic. In this study, we explore the effects of climate and terrain factors on the area of lakes in the Northwest Territories, Canada. We used the Landsat satellite archive to map interannual changes in 5,328 lakes and ponds in the Lower Mackenzie Plain between 1985 and 2020. The high temporal resolution of our dataset allowed us to classify gradual and abrupt changes in lake area and identify rapid drainage events. We used Generalized Additive Models and Random Forests to test the effects of climate and terrain factors on changes in lake area. Despite increases in the area of smaller lakes driven by increasing precipitation, we found that the total lake area has decreased by approximately 1%. Overall, 29% of lakes exhibited an increasing trend in the area, while 11% exhibited a decreasing trend, and the majority of these changes (65%) were non-linear in nature. Lakes located in fire scars were also 3.8 times more likely to show a decreasing trend in area. Analysis of a large fire indicates that lakes within the burned region exhibited declines in an area that persisted until the end of the study period 20 years after the fire. These declines are likely related to the impact of fire on thaw depth, groundwater connectivity, and the development of new drainage pathways. Our results highlight the importance of rapid drainage and wildfire as drivers of declines in the lake area.

Plain Language Summary We assessed how climate and terrain factors influence changes in the area of lakes in the Northwest Territories, Canada. Satellite observations showed that the overall surface area of lakes in our study region has decreased, and indicate that this change was driven by losses in larger water bodies. Smaller lakes tended to increase in area over time, likely responding to increases in precipitation. We also confirmed results from a previous study showing that lakes in regions impacted by wildfire are more likely to decrease in the area over time. We observed that declines in lake area following wildfire persisted for approximately 20 years after the fire, suggesting that wildfire is likely an important driver of change for lakes in subarctic environments underlain by permafrost.

1. Introduction

Across the circumpolar north, many regions are undergoing rapid changes in the distribution and abundance of surface water (Nitze et al., 2017; Pastick et al., 2019; Serreze et al., 2009; Smol & Douglas, 2007; Watts et al., 2012). Previous work shows that the magnitude and direction of change varies according to terrain and climate factors (Nitze et al., 2017; Pastick et al., 2019). In the western Canadian Arctic, surface water has shown net declines in some areas (Campbell et al., 2018; Lantz & Turner, 2015), but has been stable or increasing in others (Olthof et al., 2015; Plug et al., 2008). Understanding the rate and spatial pattern of these changes is important because wetlands, lakes, and small ponds play an important role in global climate systems (Anthony et al., 2018; Hinkel et al., 2003; Schuur et al., 2015). At a regional scale, water bodies are also a source of fresh water and provide habitat for a range of culturally and ecologically significant species (Arp et al., 2016; GRRB, 2018).

Climate and terrain characteristics influence the magnitude and direction of change in the surface area of lakes and ponds at high latitudes (Arp et al., 2012; Marsh et al., 2009; Pohl et al., 2009; Yoshikawa & Hinzman, 2003). In the high Arctic, declines in lake area have been associated with rising air temperatures and evaporative drying in small ponds (Campbell et al., 2018; Smol & Douglas, 2007). In regions of ice-rich permafrost, decreases in lake area have also been associated with thermokarst lake drainage, driven by increases in temperature and precipitation (Lantz & Turner, 2015; Nitze et al., 2020; Smith et al., 2005). Some studies have found little correlation between climate variables and changes in the lake area, suggesting that the effects of climate are mediated by terrain factors (Carroll & Loboda, 2018). Terrain characteristics likely to influence surface water dynamics include

landscape position (Nitze et al., 2017; Roach et al., 2013), ground ice content (Jones et al., 2020; Swanson, 2019; Yoshikawa & Hinzman, 2003), vegetation (Turner et al., 2014), and surficial geology (Carroll & Loboda, 2018; Nitze et al., 2017; Roach et al., 2013; Wang et al., 2018; Yoshikawa & Hinzman, 2003). These terrain characteristics also strongly influence the prevalence of thermokarst processes, which can drive both lake expansion and drainage (Kokelj & Jorgenson, 2013). Rising air temperatures, changes in the intensity of precipitation, and more frequent wildfires are also increasing the frequency of thermokarst disturbances across the circumpolar (Becker & Pollard, 2016; Gibson et al., 2018; Jones et al., 2015; Narita et al., 2015). Roach et al. (2013) found that lakes in areas affected by boreal wildfire were 1.5 times more likely to show a decreasing trend in the area. Recent evidence that thermokarst disturbances and fire are increasing in frequency and intensity highlights the need to better understand interactions between climate change, fire, permafrost conditions, and surface water dynamics (Jones et al., 2015; Kasischke & Turetsky, 2006; Nitze et al., 2020).

To understand changes in the area of lakes and ponds, previous remote sensing studies have compared lake area across two to four time-periods (Jones et al., 2011; Lantz & Turner, 2015; Lindgren et al., 2021; Marsh et al., 2009; Plug et al., 2008). Unfortunately, variation at interannual and seasonal scales, particularly in small water bodies, means that this approach may not be sensitive to the full range of changes in surface water (Carroll & Loboda, 2018; Cooley et al., 2019). Other analyses address these challenges using temporally dense image stacks to capture per-pixel trends in water coverage over large areas (Campbell et al., 2018; Nitze et al., 2017; Pastick et al., 2019; Swanson, 2019). However, inferring mechanisms of lake-level changes using conventional approaches to detect linear trends may mask rapid non-linear processes (such as rapid lake drainage) common in northern regions (Jones & Arp, 2015; Mackay, 1988; Nitze et al., 2020). In areas of ice-rich permafrost, abrupt non-linear changes in the area of lakes and ponds can be driven by thermokarst processes that may not be well represented by linear per-pixel trends in water coverage (Jones & Arp, 2015; Nitze et al., 2020).

In this study, we examined changes in the area of 5,328 lakes and ponds within the Lower Mackenzie Plains, NWT from 1985 to 2020 using 32 scenes from the Landsat satellite image archive. Prior inspection of oblique air photos and satellite imagery suggested that drained lake basins and other lake area changes were common in this region. Our goal was to quantify the overall direction and magnitude of surface water gains and losses and to investigate how climate and terrain attributes influenced observed changes. To accomplish this, we used a statistical approach to classify lakes based on the direction (+/−) and nature (linear/non-linear) of trends in surface water area. We used Generalized Additive Models to compare the effects of spring and summer temperature and precipitation on the area of large and small lakes. Random Forests were used to associate increasing and decreasing trends in lake area with several terrain variables. To assess the importance of non-linear changes in surface water, we also examined the timing of abrupt shifts in lake area following wildfire.

2. Methods

2.1. Study Area

The Lower Mackenzie Plain is located in the Northwest Territories, Canada, south of the Mackenzie Delta (Figure 1). This region is characterized by thousands of small lakes, peatlands, and spruce forests (Ecosystem Classification Group, 2009). The region is within the Gwich'in Settlement Area and includes the Gwichya Gwich'in community of Tsiigehtchic (Heine et al., 2001). Surficial geology in this region is complex and is mainly comprised of a patchwork of morainal deposits, with silty lacustrine deposits and organic peatlands adjacent to the Mackenzie River (Figure 2a). Fine Lacustrine plains are generally composed of silt and clay and overlain by discontinuous organic deposits, while morainal deposits are composed of coarse bouldery till (Aylsworth, 2000).

The Mackenzie River flows through the middle of the 14,631 km^2 study area and divides two distinct ecoregions: the Arctic Red Plain and the Travaillant Uplands (Ecosystem Classification Group, 2009). The Arctic Red Plain is located at lower elevations adjacent to the Mackenzie River and contains black spruce forest and upright shrublands interspersed with extensive peatlands (Ecosystem Classification Group, 2009). The Travailliant Upland is located at higher elevations and are characterized by white spruce forests underlain by bedrock and a thin veneer of glacial till (Ecosystem Classification Group, 2009). Wildfire is common across the study area, with 41% of it having been burned since 1965 (Figure 2b).

Monthly air temperature and precipitation data from 1985 to 2014 from the Fort McPherson airport (67°26'00N, 134°53'00W) were obtained from Environment and Climate Change Canada (ECCC, 2020). No precipitation

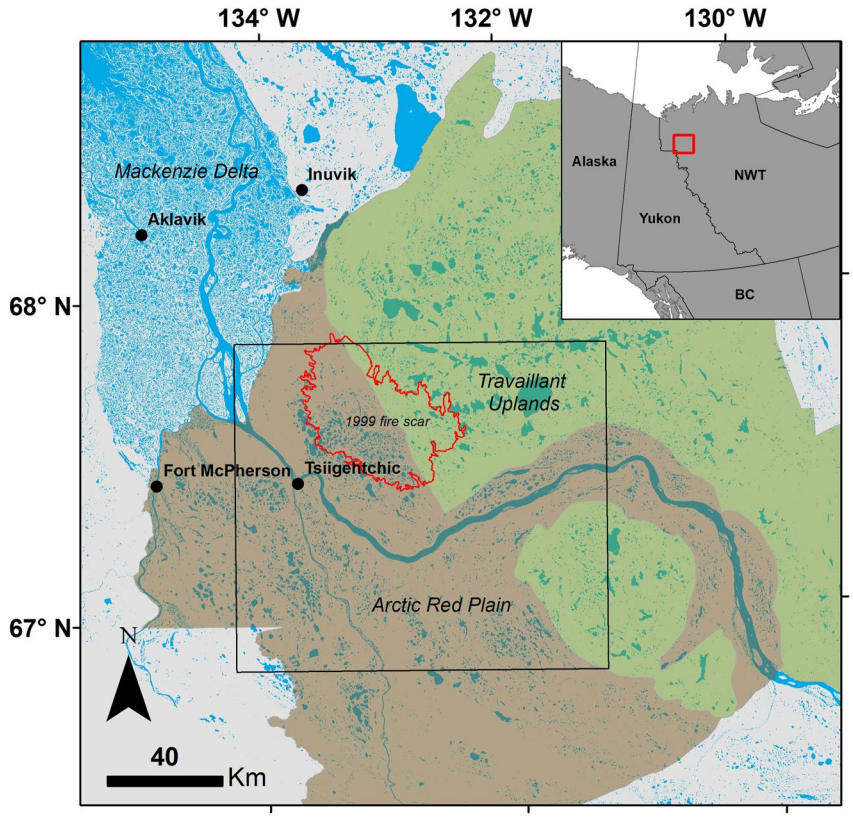

Figure 1. Study area map of the Lower Mackenzie Plains, NWT. The black outline shows the extent of the study region. The brown shaded area shows the Arctic Red Plain ecoregion and the green shaded area represents the Travaillant Uplands ecoregion. The red outline shows the boundary of a 1999 fire scar. The inset map in the upper right shows the location of the study region within northwestern Canada.

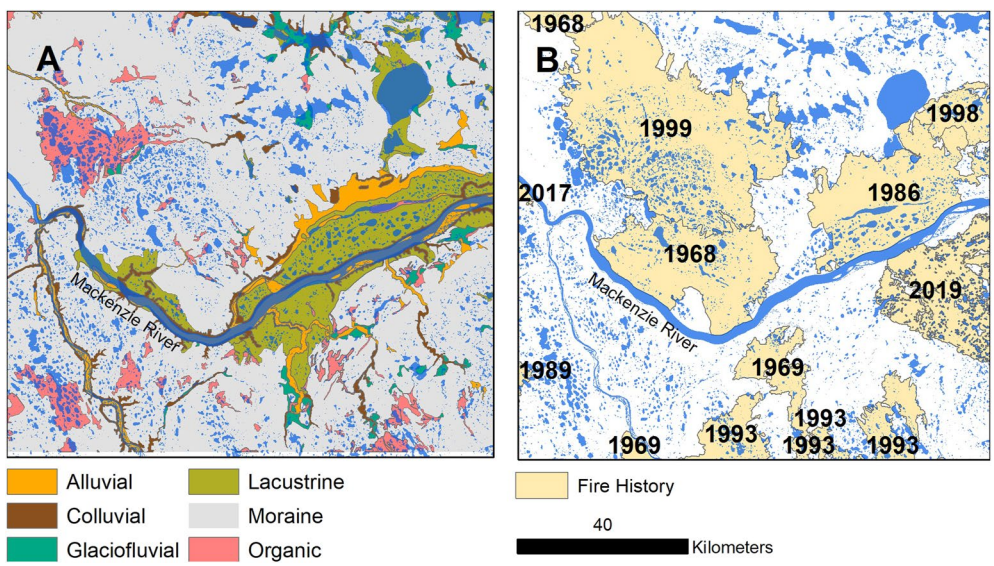

Figure 2. Maps showing surficial geology (a) and fire history (b) within the study area (black box in Figure 1). Surficial geology data is from Aylsworth et al., (2000) and fire history data are from the NWT Centre for Geomatics (2020). Dates show the timing of fires within the study region.

Table 1
The Distribution of Lake Size Classes and Total Lake Area Within Each Size Class Measured as the Sum of Average Lake Area Between 1985 and 1990

Lake size class	N	Total area (km^2)
Small (<0.05 km^2)	1193	39.84
Medium (0.05–0.5 km^2)	1758	258.50
Large (>0.5 km^2)	213	245.20

data were available between 2014 and 2020, so our analysis of climate trends was restricted to 1985–2014. The climate of this region is cold, with a mean annual air temperature of −6.7°C from 1985 to 2014. Median total annual precipitation between 1985 and 2014 was 134.4 mm per year, with a median of 104 mm falling within the June to August period. Trends in temperature and precipitation over this period indicate warming in the winter and spring, and increases in precipitation in every season except winter (Figures S1 and S2 in Supporting Information S1).

2.2. Landsat Satellite Image Processing

Data from Landsat Collection 1, which includes Landsat-5, Landsat-7, and Landsat-8, were used to quantify trends in surface water from 1985 to 2020 (Dwyer, 2019). We used Tier 1 Top-of-Atmosphere (TOA) scenes (n = 32) which are geometrically and radiometrically calibrated for use in time-series analysis (Dwyer, 2019). We did not use Surface Reflectance data due to known issues with this product at high latitudes (Jenkerson, 2019). Scenes impacted by the Landsat-7 scan line corrector failure beginning in 2003 were also excluded from our analysis. To ensure snow-free conditions, consistency in seasonal water levels and atmospheric constituents across the time series, we filtered data to only include scenes from July and August. We preferentially selected scenes within a one-month window representing mid-summer conditions between July 15 and August 15, and 60% of scenes fell within this period. In each image, we masked pixels impacted by clouds and cloud shadows using the Quality Assessment Band. After removing clouds and cloud shadows, each scene was visually inspected and discarded if smoke or clouds remained in the study area. All Landsat image pre-processing steps were performed in Google Earth Engine.

To map annual surface water coverage, we used the histogram breakpoint method developed by Olthof et al. (2015). This method quantifies the proportion of a pixel covered by water (sub-pixel water fraction) by interpolating between thresholds in the shortwave infrared reflectance band (SWIR1) representing pixels containing pure land and pure water. For a detailed description and validation of the method, see the Supporting Information S1. Next, we created a mask representing the maximum area of all water bodies in the study area. The maximum area was defined using pixels where sub-pixel water fraction was greater than 50% in two or more years. Subsequently, lake objects were created by transforming the maximal water area raster into polygon features. We used an initial threshold of 30,000 m^2 (0.03 km^2) equal to approximately 33 Landsat pixels, to filter out small ponds that were likely to have high mapping error, retaining 5,328 water bodies in the study area.

2.3. Changes in Lake Area

We assessed changes in total lake area as well as changes within individual lakes. First, we estimated the total lake area using lakes with less than 10 missing observations (due to cloud or smoke cover) across the time series (n = 3,164/5,328). To estimate the change in water area over time, we calculated a 5-point moving average for each lake. This process helped to fill gaps where lakes may have been covered by clouds or smoke in an individual Landsat scene. The resulting dataset was comprised of a moving average of lake area across five consecutive Landsat acquisitions. We calculated the total lake area as the sum of lake area within these 5-point time periods. To ensure that the same population of lakes was represented in each period, we omitted periods with missing data resulting from lakes having no available data for five consecutive Landsat acquisitions. Changes in total lake area were also analyzed using the following size classes: 1) large lakes (>0.5 km^2), medium lakes (0.05–0.5 km^2), and small lakes (<0.05 km^2) based on the average area between 1985 and 1990 (Table 1).

To assess changes in the area of individual lakes, we tested for trends over time and classified lakes using two criteria: (a) the direction of change and (b) whether changes were linear or non-linear over time. To test for trends, we used the Mann Kendall Trend Test to determine if the lake area exhibited a monotonic increase, decrease, or non-significant trend in the area over time. We used the Kendall package in R to calculate Kendall's Tau statistic and corresponding p-value for each lake (McLeod, 2011). Lakes with a p-value <0.1 were classified as either increasing or decreasing depending on the sign of the Tau statistic, and lakes with p-value >0.1 were classified as non-trended. Next, we used Generalized Additive Models (GAM) to classify trends as either linear or non-linear over time. We fit a GAM to the area of each lake over time and extracted the Estimated Degrees of Freedom

(EDF) using the R package mgcv (Wood, 2017). The EDF indicates the number of knots in the smooth effect of time in the model and provides a measure of the 'wiggliness' of the fitted model. Large values indicate a strong non-linear relationship over time and values close to one indicate a linear fit. Lakes with EDF greater than 1.1 were classified as non-linear and EDF less than 1.1 were classified as linear. The results of these two tests were combined to classify each lake into one of the six change classes (increasing vs. decreasing and non-trended and linear vs. non-linear) shown in Figure S5 in Supporting Information S1.

To identify rapid drainage events in large and medium sized lakes we used breakpoint regression from the strucchange package in R (Zeileis, 2004). We used the breakpoints function to compute the location of breaks, which represent the transition from one stable linear regression relationship to another, and are calculated using the algorithm described in Bai and Perron (2003). We did not identify rapid drainage events in small lakes as they represent a small (~6%) proportion of the total lake area and the potential for misclassification in the area of small lakes is greater. We selected lakes exhibiting one breakpoint, a decreasing trend in the area, and change exceeding 30% relative to its initial area (average area between 1985 and 1990). The 30% threshold has previously been used to identify catastrophic lake drainage in other regions (Hinkel et al., 2007; Lantz & Turner, 2015). To distinguish between lakes exhibiting rapid drainage from other drying processes, including evaporation (gradual linear change) or bi-directional change, we examined the time-series of each lake matching these criteria. We considered lake drainage to be rapid if the lake lost at least 30% of its initial area within one year.

We also used breakpoint regression to examine the effect of a large fire that burned in 1999 on initiating abrupt changes in the lake area. The fire covered 1,632 km^2 and 836 lakes were completely contained within the fire boundary. This fire was selected because its large size and timing allowed us to obtain a large sample of lakes inside and outside the fire, and to assess change before and after the burn. To test the hypothesis that forest fires can initiate non-linear changes in lake area, we compared the frequency and timing of breakpoints in the surface area time series for burned lakes and lakes within 10 km of the fire scar. We also compared interannual change in lake area between burned and unburned lakes.

2.4. Climate Models

We tested hypotheses relating the effects of spring and summer climate on changes in total lake area using Generalized Additive Models and climate data from the Fort McPherson airport between 1985 and 2014 (Environment and Climate Change Environment Canada, 2020). We used data from May and July to capture spring and summer conditions because data for these months comprised the most complete daily record over the period of study (Figure S3 in Supporting Information S1). Months with more than 10 days of missing data were removed from the analysis. We hypothesized that small lakes would be more responsive to variation in May and July climate conditions compared to large lakes, due to their greater surface area to volume ratios (Marsh & Bigras, 1988). We fit separate models for large and small lakes and compared the magnitude and significance of the climate parameters. In this analysis, we calculated lake area over time using a sample of large ($n = 17$) and small lakes ($n = 215$) and Landsat acquisitions ($n = 12$) with no missing data. This subset of the data represents lakes completely unaffected by cloud cover and ensures that estimates of total annual lake area were calculated on the same population of lakes in each year of the time series. We removed lakes from analysis if they were identified as having undergone rapid drainage. Total lake area was aggregated by lake size and we fit Generalized Additive Models using the R package mgcv (Wood, 2011). In both models (large and small lakes), total lake area (km^2) was fit as the response variable and the number of days since the beginning of the time series was modeled as a non-linear smooth effect. To avoid overfitting on a small dataset we set a low basis dimension for the smoothed term ($k = 3$). Total May precipitation, mean May temperature, total July precipitation, mean July temperature, and the month of the Landsat acquisition (July or August), were fit as linear effects. To account for temporal autocorrelation in the data we modeled a correlation structure by including a first order autoregressive term. To validate these models we examined plots of model residuals and autocorrelation using the acf function in R (R Core Team, 2020). The intercept parameter in both models represents the annual lake area in kilometers at the beginning of the time-series, if all coefficients are set to 0.

Table 2
Terrain Variables Included in the Random Forests Model to Predict the Direction of Change in Lake Area (Increasing or Decreasing)

Variable	Description/Source	Rationale
Ecoregion	Classification of level 4 ecoregions in the Taiga Plains (NWT Ecosystem Classification Group, 2009)	Vegetation, geology and other landscape characteristics likely influence lake expansion and drainage.
Surficial geology	Surficial geology of the Fort McPherson region (Aylsworth, 2000)	Soil texture influences permeability and rate of drainage with lakes in coarse-grained sand more likely to decrease in area (Wang et al., 2018).
Lake Area	Average lake area between 1985 and 1990	Smaller lakes may be more susceptible to evaporative drying and trends in precipitation (Campbell et al., 2018).
Fire history	Boundaries of recent wildfires from 1965 to 2019 (NWT Centre for Geomatics, 2020).	Lakes in fire scars are more likely to decrease in area due to increased connectivity to groundwater following fire (Roach et al., 2013).
Drainage gradient (Slope)	Mean slope within 30m of lake perimeters calculated using the Arctic DEM data (Porter et al., 2018).	Lakes at low elevation relative to surroundings may be more likely to increase in area.
Interlake Distance	Distance to nearest neighboring lake measured using lake perimeters.	Lakes that tap other nearby water bodies may be more likely to drain.

2.5. Random Forests

To further explore the drivers of lake area change and the relative importance of terrain variables, we used a Random Forests model to classify lakes showing increasing and decreasing trends in area (Breiman, 2001). The explanatory variables used in this model are described in Table 2. Random forests models were created in R using the randomforests package and each tree was trained on a balanced sample of increasing and decreasing lakes (Liaw & Wiener, 2002). We estimated the relative importance of terrain variables using the unscaled mean decrease in accuracy, and partial dependence plots to visualize the marginal effects of each variable on classification probability (Liaw & Wiener, 2002). Partial dependence plots were created using the pdp package in R (Greenwell, 2017).

In addition to the R packages cited previously, figures throughout the paper were created using the ggplot2 package (Wickham, 2016). A range of helper functions from the packages dplyr (Wickham & Henry, 2020) tidyr (Wickham et al., 2020), data.table (Dowle & Srinivasan, 2019), gmodels (Warnes et al., 2018) and zoo (Zeileis & Grothendieck, 2005) were also used to process and clean the data for analysis.

3. Results

3.1. Overall Change in Lake Surface Area

Between 1985 and 2020, 43% of lakes showed a significant trend in area, and the majority of these changes (65%) were non-linear in nature. Total lake area in the study region decreased by approximately 1%, representing a net change of 5.18 km^2 (Figure 3). Declines in total lake area primarily occurred early in the time series (between

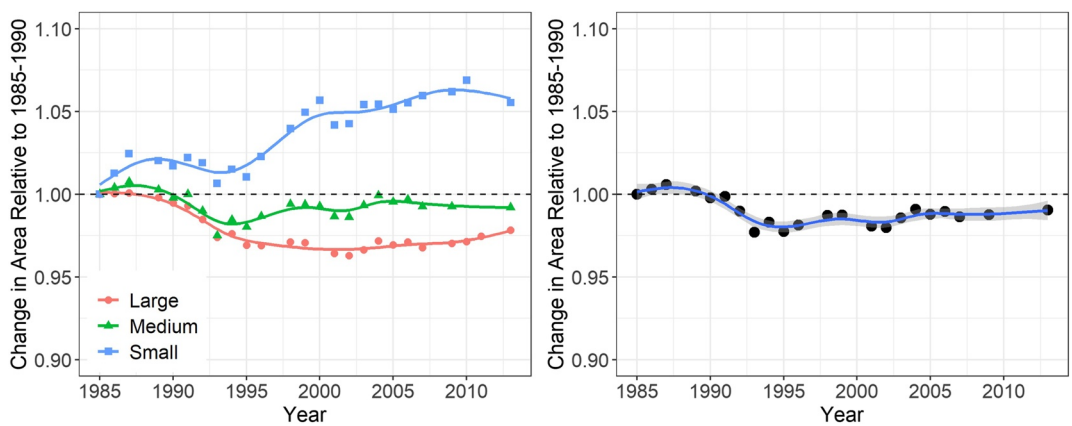

Figure 3. Change in total lake area relative to the average area between 1985 and 1990 by lake size (left) and total lake area (right). Data in the time series represents a 5-point moving average.

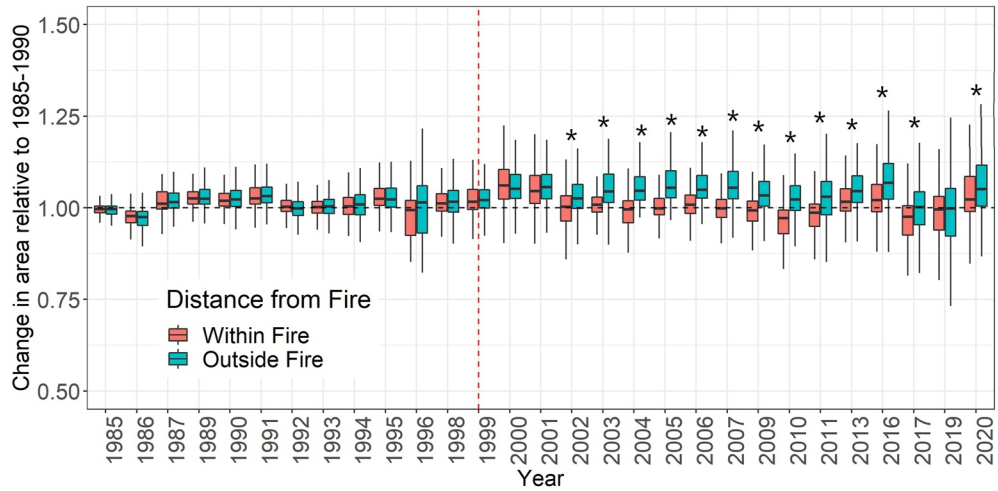

Figure 4. Boxplots comparing the median change in lake area relative to the average area between 1985 and 1990 for lakes within a fire scar and lakes outside the fire but within 10 km of the fire boundaries. The extent of the box shows the interquartile range and the whiskers show the 10th and 90th percentiles. The dashed vertical line shows the year the fire occurred. Landsat imagery from 1999 was captured prior to the fire. Asterisks (*) indicate a statistically significant difference at the $p < 0.01$ level.

1985 and 1995) and remained relatively stable for the rest of the time series. The total area of large and medium sized lakes both declined over time (Figure 5), while the total area of small lakes increased by approximately 5%. Mann Kendall Trend tests show that the majority (57%) of lakes did not show a significant change in area over time, but 29% of lakes showed a significant increasing trend and 13% showed a decreasing trend (Table 3). Lakes exhibiting significant changes in the area tended to show primarily non-linear changes (Table 3).

3.2. Identifying Rapid Lake Drainage

We identified 13 large lakes and 38 medium sized lakes exhibiting large non-linear decreases in area, indicative of rapid drainage. Inspection of each lake time series showed that the majority of these lakes exhibited bi-directional change and did not drain permanently. Based on patterns in the time-series we identified five lakes (two large and three medium sized lakes) showing rapid and persistent drainage (Figure S6 in Supporting Information S1). This suggests that over the 35-year time series, the annual rate of rapid drainage events among lakes larger than 0.05 km^2 was 0.14 lakes per year. The five lakes that drained over this period account for 1.41 km^2 of surface water loss, or 27% of total surface water loss. Two of these lakes (accounting for 14% of total water loss) were located in the 1999 fire and drained rapidly within 3 years of the fire (Figure S6 in Supporting Information S1).

3.3. Effect of 1999 Fire on Lake Area Trends

Our analysis shows that 33% of lakes inside the region burned by a 1999 fire exhibited a significant decrease in surface area compared to 5% of lakes within 10 km of the fire. One-sided Mann Whitney tests show that lakes inside the fire had significantly lower relative area compared to lakes outside the fire ($p < 0.01$) for 13 out of the 16 years after the fire, but never before the fire (Figure 4). The relative area of lakes within the fire was still significantly lower than unburned lakes in 2019, 20 years after the fire occurred in 1999 (Figure 4). Breakpoint regression analysis shows that the frequency of breakpoints for lakes inside and outside the burned area was similar before the fire, but increased for lakes inside the burned area immediately after the fire (Figure 5). The largest difference in breakpoint frequency occurred in 2001 when 22% of burned lakes showed a breakpoint compared to only 2% of unburned lakes (Figure 5). After 2001, the difference in breakpoint frequency between burned and unburned lakes was less than 1% for all years except 2007 (6% difference).

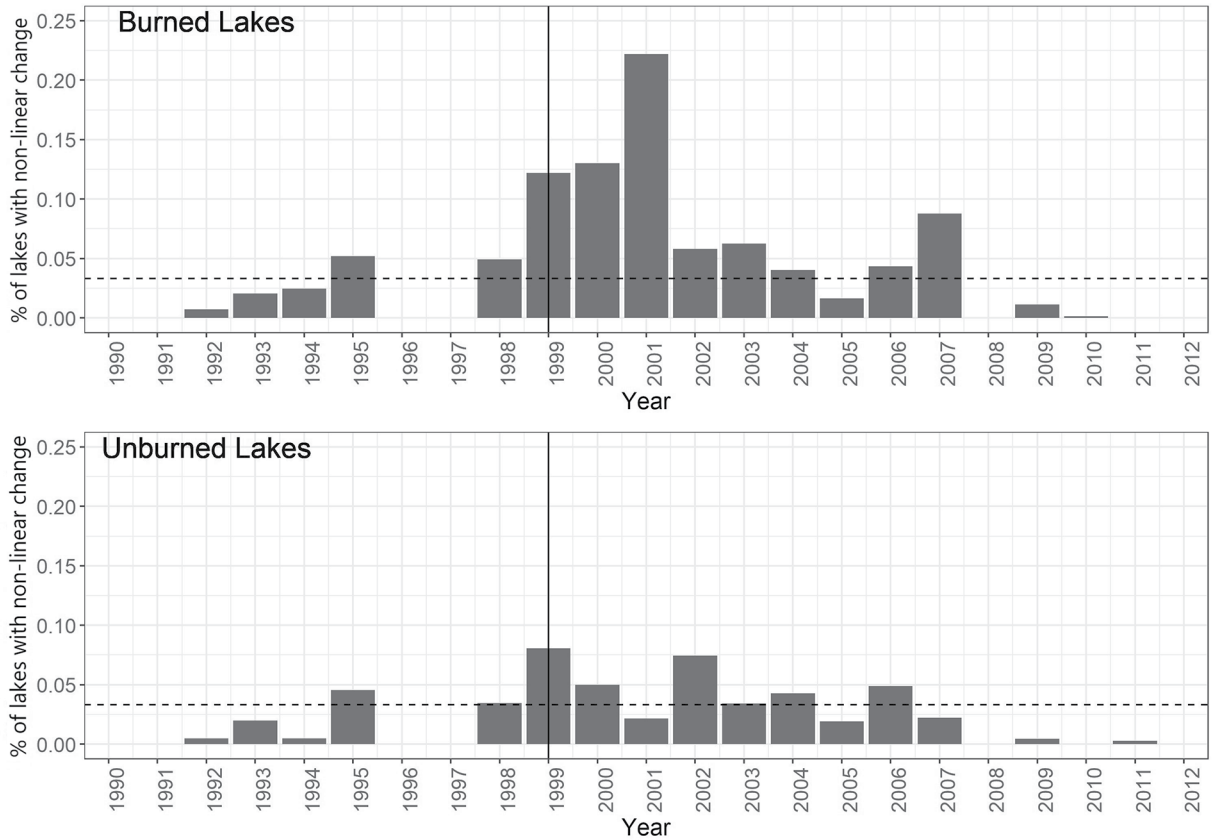

Figure 5. Comparison of the frequency of breakpoints in the time series of lake area for lakes within a large burned area (top, $n = 836$) and lakes within 10 km of the fire scar (bottom, $n = 752$). Note that no data were available for 1996, 1997, and 2008. The solid black line shows the year of the fire and the dashed horizontal line shows the average proportion of lakes with a breakpoint for all lakes in the study area.

3.4. Effect of Spring and Summer Climate Variables on Total Lake Area

Generalized additive models relating interannual variability in lake area with climate variables showed that July precipitation had a significant positive effect on total lake area for both large and small lakes (Table 4). The effects of May and July temperature and May precipitation were not significant in either model (Table 4). The non-linear smooth effect for time and the effect of month was significant for large lakes, with lake area in August lower on average than lake area in July.

3.5. Association Between Lake Area Trends and Terrain Type

The unscaled variable importance for the random forests classification shows that the most important predictors of the direction of change in lake area were initial lake area, fire history, and surficial geology (Figure 6). Partial dependence plots showing the probability of a lake being classified as increasing versus decreasing in area indicate that smaller lakes, lakes outside of fire scars, and lakes in fine-grained lacustrine deposits were most likely to increase in area over time (Figure 7). Conversely, larger lakes, lakes within fire scars, and lakes in organic deposits were more likely to decrease in area (Figure 7). The random forests classification showed 72.4% accuracy and a kappa score of 0.38, indicating a fair agreement between model predictions and actual trend classes (Landis & Koch, 1977).

Table 3
Percent of Lakes in the Study Area Belonging to Six Drainage Classes Based on a Mann Kendall Trend Test to Determine the Direction of Change (Increasing, Decreasing or Non-Trended) and a Generalized Additive Model to Determine the Nature of Change (Linear or Non-linear)

	Increasing	Decreasing	Non-trended	Total
Linear	11%	4%	19%	34%
Non-Linear	18%	10%	38%	66%
Total	29%	14%	57%	N = 5328

Table 4
Parameter Estimates From Generalized Additive Models of Total Lake Area as a Function of Month, Lake Size and May and July Climate Variables

Large lakes				
$r^2 = 0.874$				
Parametric Coefficients	**Estimate**	**Std.Error**	**t-value**	**p-value**
Intercept	13.770	0.905	15.220	0.000***
Acquisition month (Aug)	−1.076	0.200	−5.371	0.006***
May Precip (mm)	0.015	0.008	1.746	0.155
May Temp (°C)	0.057	0.05	1.139	0.318
July Temp (°C)	0.007	0.061	0.122	0.909
July Precip (mm)	0.020	0.004	4.508	0.012**
Smooth term	**Edf**	**---**	**f-value**	**p-value**
Date	1.989	---	41.11	0.001***
Small Lakes				
$r^2 = 0.669$				
Parametric Coefficients	**Estimate**	**Std.Error**	**t-value**	**p-value**
Intercept	6.984	0.411	16.983	0.000***
Acquisition month (Aug)	−0.178	0.090	−1.973	0.118
May Precip (mm)	0.006	0.004	1.642	0.174
May Temp (°C)	0.016	0.023	0.722	0.509
July Temp (°C)	0.003	0.028	0.095	0.928
July Precip (mm)	0.008	0.002	4.087	0.014**
Smooth term	**Edf**	**---**	**f-value**	**p-value**
Date	1.891	---	3.337	0.109

Note. Estimates of parametric coefficients represent the change in total lake area in km^2 per unit increase in each explanatory variable. The effect of acquisition month represents the mean difference in lake area between July and August acquisitions. The effective degrees of freedom (EDF) of the smooth term represents the number of knots in the smoothed parameter, where values close to 1 indicate that the parameter was modeled as a linear effect. Asterisks denote statistically significant results at the $p < 0.1$ (*), $p < 0.05$ (**) and $p < 0.01$ (***) level.

4. Discussion

Our analysis shows that changes in Subarctic surface water are influenced by lake size, climate, and terrain factors, but also highlights that wildfire can have a disproportionate influence. Drainage of two large lakes following a 1999 fire accounted for 14% of total water loss in the study area and the majority (79%) of lakes showing decreasing trends were located within burned areas. Roach et al., (2013) also observed that lakes inside burned areas were more likely to decrease in the area over time. Observed decreases in lake size within fire-impacted areas were likely caused by increased ground heat flux and active layer deepening following the combustion of vegetation and surface organics. Observations at Arctic and sub-Arctic sites show that reduced organic layer depth, lower surface albedo, and increased thermal conductivity following fire all contribute to long-term increases in active layer depth (Liljedahl et al., 2007; Yoshikawa et al., 2002; Zipper et al., 2018). Active layer deepening can increase soil water storage capacity and increase hydrological connectivity, and connectivity to groundwater, impacting both inflow and outflow to a lake (Haynes et al., 2019; Jones et al., 2020; Liljedahl et al., 2007; Roach et al., 2013). Lakes with decreasing trends in area were more likely to show non-linear change rather than linear change, which likely reflects the prevalence of rapid lake drainage as well as bi-directional changes resulting from partial lake infilling. It is also possible that the rapid drainage of the two large lakes following the 1999 fire was caused by changes in near-surface ground ice conditions and the formation of new outlet channels (Nitze et al., 2020; Yoshikawa et al., 2002). To investigate the geophysical mechanisms driving these changes, future work could pair remote sensing observations with measurements of ground temperature and active layer depth. Other forms of remote sensing data such as repeated LiDAR surveys and thermal imaging would also help map changes in permafrost conditions and ground temperature following fire. Understanding the interaction between permafrost, fire, and lake area is important given the increasing frequency and size of northern wildfires (Hu et al., 2015; Kasischke & Turetsky, 2006). Persistent declines in lake area following fire will likely have long-term impacts on ground temperatures, permafrost aggradation (Burn, 2005) as well as vegetation succession, and habitat quality in drained areas (Cooley et al., 2020; Lantz, 2017; Marsh et al., 2009).

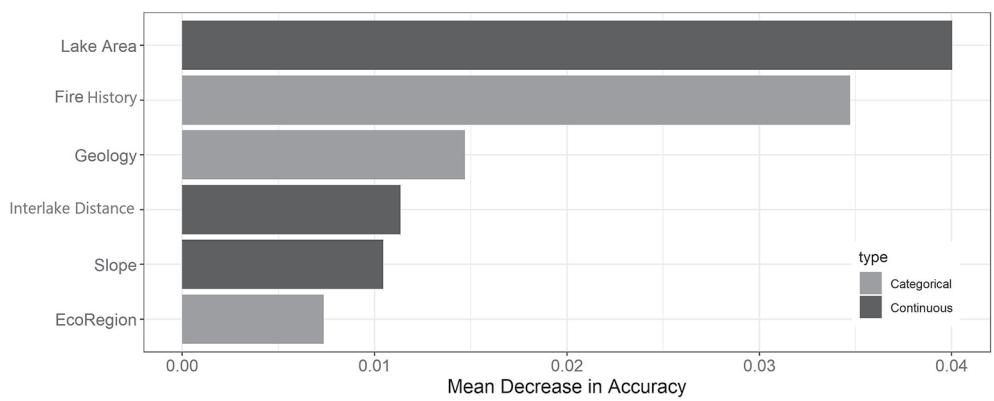

Figure 6. Variable importance plot from the Random Forests Model of lake-trend type (increasing vs. decreasing). Unscaled variable importance shows the mean decrease in model accuracy if that variable is excluded.

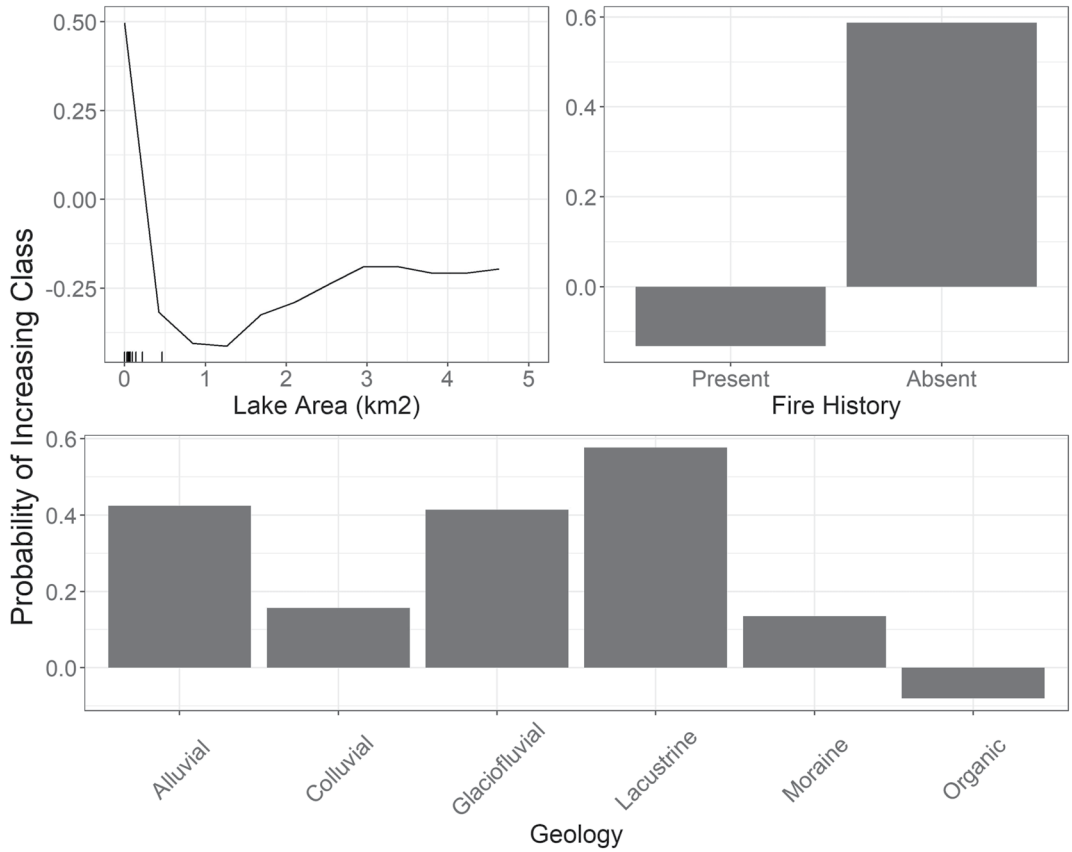

Figure 7. Partial dependence plots showing the probability of observing increasing surface water area versus decreasing area as a function of the three most important independent variables in the random forests model: (a) lake area, (b) fire presence/absence (c) surficial geology. Negative probability values indicate that increases in the area were less likely compared to decreases at that value of the independent variable. Rug marks show the deciles of the lake area data, (to better represent partial dependence for the majority of lakes, note that lakes larger than 5 km^2 were included in the model but not plotted).

The strong relationship between interannual variation in lake area and July precipitation indicates that climate can also influence lake area. Despite the fact that summer precipitation and the number of large rainfall events increased between 1985 and 2020, total surface water in the study area decreased by 1%. A change that was largely driven by declines in large and medium sized lakes (Figure 3). This suggests that precipitation increases were not the primary control of net change in lake area over the interval studied. Attempts to predict the direction of change in lake area in other regions should consider local terrain and permafrost characteristics that may mediate the effects of climate change**.** While the area of both large and small lakes showed a significant positive relationship with July precipitation, only small lakes experienced an overall increase in surface area (Figure 3). The greater sensitivity of small lakes to increased precipitation in the study region may have been driven by their greater surface area to volume ratios (Arp et al., 2011; Campbell et al., 2018; Marsh & Bigras, 1988), however, field data on lake depth is needed to confirm this hypothesis. Greater sensitivity to climate change among small lakes and ponds has also been reported in the Arctic and sub-Arctic where decreases in lake area have been attributed to evaporative drying (Campbell et al., 2018; Carroll & Loboda, 2018; Smith et al., 2005; Smol & Douglas, 2007). The observed 1% decrease in total lake area in our study region, is also comparable to other regions. Similar studies in Old Crow Flats and interior Alaska showed a 5% and 3% decrease in total lake area (Lantz & Turner, 2015; Rover et al., 2012). Change in our study area was likely smaller because of increases in small lakes and the frequency of lakes that partially drained and subsequently refilled. Differences in the time-period analyzed may have also influenced the magnitude of observed changes.

Our analyses suggest that decreases in lake area were also facilitated by differences in surficial materials across the study area. Random Forests showed that lakes underlain by organic material were the most likely to show decreasing trends in area, and lakes in fine-silty lacustrine sediments were more likely to show increasing trends

(Carroll & Loboda, 2018; Wang et al., 2018). Decreases in the number and size of thermokarst lakes have been observed in areas with coarse soil texture and permeable sand deposits, while less permeable silt deposits have been associated with increasing lake area (Carroll & Loboda, 2018; Wang et al., 2018). Soil texture also influences ground-ice content, which may contribute to the frequency of thermokarst lake drainage (Jorgenson et al., 2008; O'Neill et al., 2019).

Our data also show that rapid lake drainage is an important hydrological process in our study area. Five rapid drainage events among lakes larger than 0.05 km^2 accounted for 27% of total lake area loss. Rapid catastrophic lake drainage has been reported as a significant driver of change in many ice-rich permafrost environments (Jones & Arp, 2015; Lantz & Turner, 2015; Mackay, 1988; Nitze et al., 2020). Rapid lake drainage can occur through a range of thermokarst processes resulting in head-ward erosion, or the formation of a new outlet channel. We observed a rate of 0.14 rapid drainage events per year. This is lower than rates reported in studies focused on Alaska and the Tuktoyaktuk Coastal Plain where average drainage rates were 1.6 and 0.33 lakes per year over a similar time period (Jones et al., 2020; Marsh et al., 2009). Due to missing data for some lakes, we could not confirm if some drainage events occurred within a 1-year period, thus our estimate of the rate of catastrophic drainage events is likely conservative. In other regions, large decreases in lake area typically corrrespond to permanent losses (Lantz & Turner, 2015; Nitze et al., 2020), however, in this region, we observed that large losses in lake area were frequently followed by partial refilling.

5. Conclusions

In this analysis, we used the Landsat satellite archive to map interannual changes in the area of 5,379 lakes in the Lower Mackenzie Plains between 1985 and 2020. We found a small decrease in the total lake area, despite increases in summer precipitation. Lake size had a strong effect on the direction of change, with smaller lakes more likely to increase in area and larger lakes more likely to decrease in area. Sediment permeability also influenced the direction of change, with lakes located in fine-grained lacustrine sediment more likely to increase in area compared to lakes in more permeable organic deposits. We also show that 27% of all lake area losses in the study area were associated with the rapid drainage of five large and medium sized lakes. This suggests that thermokarst processes are an important contributor to lake area change in this region. In particular, lakes located in fire scars were 3.8 times more likely to show a decreasing trend in the area. These results are similar to those reported in Roach et al. (2013), however, more work is needed to understand the physical mechanisms linking wildfire to lake area change. While a small subset of lakes showed permanent losses in the water area, partial infilling of drained lakes was also common. At the local scale, these changes are likely to impact permafrost aggradation, wildlife habitat, and vegetation succession (Burn, 2005; Cooley et al., 2020; Lantz, 2017; Marsh et al., 2009). Across broader spatial scales, understanding the direction of change in lake area will be important in predicting the response of permafrost to climate change and greenhouse gas emissions from permafrost soils (Anthony et al., 2014).

Data Availability Statement

Data used in this study are publicly available from the cited literature. Images from the Landsat satellite archive were downloaded through Google Earth Engine (Google Earth Engine). Historic climate data from Fort McPherson is available through Environment and Climate Change Canada (Station Results - Historical Data - Climate - Environment and Climate Change Canada (weather.gc.ca)). Processed satellite images, associated shapefiles, and data derived from satellite images are available from the Scholars Portal Dataverse at https://doi.org/10.5683/SP3/MZ4XS0.

Acknowledgments
This research was funded by ArcticNet and the Natural Sciences and Engineering Council of Canada through a Discovery Grant (06,210-2018) to Trevor Lantz and a Canada Graduate Scholarship Award to Hana Travers-Smith. We also acknowledge funds and support from the University of Victoria, the Garfield Weston Foundation, the Northern Science Training Program, and the Polar Continental Shelf Project.

References

Anthony, K. M., Schneider von Deimling, T., Nitze, I., Frolking, S., Emond, A., Daanen, R., et al. (2018). 21st-century modeled permafrost carbon emissions accelerated by abrupt thaw beneath lakes. *Nature Communications*, *9*(1), 1–11. https://doi.org/10.1038/s41467-018-05738-9

Anthony, K. M. W., Zimov, S. A., Grosse, G., Jones, M. C., Anthony, P. M., Chapin, F. S., III, et al. (2014). A shift of thermokarst lakes from carbon sources to sinks during the Holocene epoch. *Nature*, *511*(7510), 452–456. Gale OneFile: CPLQ. https://doi.org/10.1038/nature13560

Arp, C. D., Jones, B. M., Grosse, G., Bondurant, A. C., Romanovsky, V. E., Hinkel, K. M., & Parsekian, A. D. (2016). Threshold sensitivity of shallow Arctic lakes and sublake permafrost to changing winter climate. *Geophysical Research Letters*, *43*(12), 6358–6365. https://doi.org/10.1002/2016GL068506

Arp, C. D., Jones, B. M., Lu, Z., & Whitman, M. S. (2012). Shifting balance of thermokarst lake ice regimes across the Arctic Coastal Plain of northern Alaska. *Geophysical Research Letters*, *39*(16). https://doi.org/10.1029/2012GL052518

Arp, C. D., Jones, B. M., Urban, F. E., & Grosse, G. (2011). Hydrogeomorphic processes of thermokarst lakes with grounded-ice and floating-ice regimes on the Arctic coastal plain, Alaska. *Hydrological Processes*, *25*(15), 2422–2438. https://doi.org/10.1002/hyp.8019

Aylsworth, J. M., Burgess, M. M., Desrochers, D. T., Duk-Rodkin, A., Robertson, T., & Traynor, J. A. (2000). *Surficial geology, subsurface materials, and thaw sensitivity of sediments [Map]*. Geological Survey of Canada.

Bai, J., & Perron, P. (2003). Computation and analysis of multiple structural change models. *Journal of Applied Econometrics*, *18*(1), 1–22. https://doi.org/10.1002/jae.659

Becker, M. S., & Pollard, W. H. (2016). Sixty-year legacy of human impacts on a high Arctic ecosystem. *Journal of Applied Ecology*, *53*(3), 876–884. https://doi.org/10.1111/1365-2664.12603

Breiman, L. (2001). Random forests. *Machine Learning*, *45*, 5–32. https://doi.org/10.1023/a:1010933404324

Burn, C. R. (2005). Lake-bottom thermal regimes, western Arctic coast, Canada. *Permafrost and Periglacial Processes*, *16*(4), 355–367. https://doi.org/10.1002/ppp.542

Campbell, T. K. F., Lantz, T. C., & Fraser, R. H. (2018). Impacts of climate change and intensive lesser snow goose (chen caerulescens caerulescens) activity on surface water in high Arctic pond complexes. *Remote Sensing*, *10*(12), 1892. https://doi.org/10.3390/rs10121892

Carroll, M. L., & Loboda, T. V. (2018). The sign, magnitude and potential drivers of change in surface water extent in Canadian tundra. *Environmental Research Letters*, *13*(4), 045009. https://doi.org/10.1088/1748-9326/aab794

Cooley, D., Clarke, H., Graupe, S., Landry-Cuerrier, M., Lantz, T., Milligan, H., et al. (2020). The seasonality of a migratory moose population in northern Yukon. *Alces: A Journal Devoted to the Biology and Management of Moose*, *55*(1), 105–130.

Cooley, S. W., Smith, L. C., Ryan, J. C., Pitcher, L. H., & Pavelsky, T. M. (2019). Arctic-boreal lake dynamics revealed using CubeSat imagery. *Geophysical Research Letters*, *46*(4), 2111–2120. https://doi.org/10.1029/2018GL081584

Dowle, M., & Srinivasan, A. (2019). *Data.table: Extension of `data.frame`. R package version 1.12.8*. Retrieved from https://CRAN.R-project.org/package=data.table

Dwyer, J. L. (2019). *Landsat Collection 1 level 1 product Definition*. Department of the Interior US Geological Survey. LSDS-1656 Version 2.0.

Ecosystem Classification Group. (2009). *Ecological regions of the Northwest Territories – Taiga plains*. Department of Environment and Natural Resources, Government of the Northwest Territories. (viii + 173 pp. + folded insert map).

Environment Canada. (2020). *National climate data and Historical Information archive*. Retrieved from https://climate.weather.gc.ca/

Gibson, C. M., Chasmer, L. E., Thompson, D. K., Quinton, W. L., Flannigan, M. D., & Olefeldt, D. (2018). Wildfire as a major driver of recent permafrost thaw in boreal peatlands. *Nature Communications*, *9*(1), 3041. https://doi.org/10.1038/s41467-018-05457-1

Greenwell, B. M. (2017). pdp: An R package for constructing partial dependence plots. *The R Journal*, *9*(1), 421–436. https://doi.org/10.32614/rj-2017-016

GRRB. (2018). *Research and Management Interests for the GSA*. Retrieved from http://www.grrb.nt.ca/pdf/Public%20registry/research/Research%20Interests_2018.pdf

Haynes, K. M., Connon, R. F., & Quinton, W. L. (2019). Hydrometeorological measurements in peatland-dominated, discontinuous permafrost at Scotty Creek, Northwest Territories, Canada. *Geoscience Data Journal*, *6*(2), 85–96. https://doi.org/10.1002/gdj3.69

Heine, M., Andre, A., Kritsch, I., & Cardinal, A. (2001). *Gwichya Gwich'in Googwandak: The history and stories of the Gwichya Gwich'in ; as told by the Elders of Tsiigehtchic*. Gwich'in Social and Cultural Institute.

Hinkel, K. M., Eisner, W. R., Bockheim, J. G., Nelson, F. E., Peterson, K. M., & Dai, X. (2003). Spatial extent, age, and carbon stocks in drained thaw lake basins on the Barrow Peninsula, Alaska. *Arctic Antarctic and Alpine Research*, *35*(3), 291–300. https://doi.org/10.1657/1523-0430(2003)035[0291:SEAACS]2.0.CO;2

Hinkel, K. M., Jones, B. M., Eisner, W. R., Cuomo, C. J., Beck, R. A., & Frohn, R. (2007). Methods to assess natural and anthropogenic thaw lake drainage on the western Arctic coastal plain of northern Alaska. *Journal of Geophysical Research: Earth Surface*, *112*(F2). https://doi.org/10.1029/2006JF000584

Hu, F. S., Higuera, P. E., Duffy, P., Chipman, M. L., Rocha, A. V., Young, A. M., et al. (2015). Arctic tundra fires: Natural variability and responses to climate change. *Frontiers in Ecology and the Environment*, *13*(7), 369–377. https://doi.org/10.1890/150063

Jenkerson, C. (2019). *Landsat 8 surface reflectance Code (LASRC) product Guide* (p. 39). USGS. LSDS-1368 Version 2.

Jones, B. M., & Arp, C. D. (2015). Observing a catastrophic thermokarst lake drainage in northern Alaska. *Permafrost and Periglacial Processes*, *26*(2), 119–128. https://doi.org/10.1002/ppp.1842

Jones, B. M., Arp, C. D., Grosse, G., Nitze, I., Lara, M. J., Whitman, M. S., et al. (2020). Identifying historical and future potential lake drainage events on the western Arctic coastal plain of Alaska. *Permafrost and Periglacial Processes*, *31*(1), 110–127. https://doi.org/10.1002/ppp.2038

Jones, B. M., Grosse, G., Arp, C. D., Jones, M. C., Anthony, K. M. W., & Romanovsky, V. E. (2011). Modern thermokarst lake dynamics in the continuous permafrost zone, northern Seward Peninsula, Alaska. *Journal of Geophysical Research: Biogeosciences*, *116*(G2). https://doi.org/10.1029/2011JG001666

Jones, B. M., Grosse, G., Arp, C. D., Miller, E., Liu, L., Hayes, D. J., & Larsen, C. F. (2015). Recent Arctic tundra fire initiates widespread thermokarst development. *Scientific Reports*, *5*. https://doi.org/10.1038/srep15865

Jorgenson, T., Yoshikawa, K., Kanevskiy, M., Shur, Y., Romanovsky, V., Marchenko, S., et al. (2008). Permafrost characteristics of Alaska. *Proceedings of the 9th International Conference on Permafrost*, *29*, 121–122.

Kasischke, E. S., & Turetsky, M. R. (2006). Recent changes in the fire regime across the North American boreal region—spatial and temporal patterns of burning across Canada and Alaska. *Geophysical Research Letters*, *33*(9). https://doi.org/10.1029/2006GL025677

Kokelj, S. V., & Jorgenson, M. T. (2013). Advances in thermokarst research. *Permafrost and Periglacial Processes*, *24*(2), 108–119. https://doi.org/10.1002/ppp.1779

Landis, J. R., & Koch, G. G. (1977). The measurement of observer agreement for Categorical data. *Biometrics*, *33*(1), 159–174. https://doi.org/10.2307/2529310

Lantz, T. C. (2017). Vegetation succession and environmental conditions following catastrophic lake drainage in Old Crow Flats, Yukon. *Arctic*, *70*(2), 177. https://doi.org/10.14430/arctic4646

Lantz, T. C., & Turner, K. W. (2015). Changes in lake area in response to thermokarst processes and climate in Old Crow Flats, Yukon. *Journal of Geophysical Research: Biogeosciences*, *120*(3), 513–524. https://doi.org/10.1002/2014JG002744

Liaw, A., & Wiener, M. (2002). Classification and regression by randomForest. *R News*, *2*(3), 18–22.

Liljedahl, A., Hinzman, L., Busey, R., & Yoshikawa, K. (2007). Physical short-term changes after a tussock tundra fire, Seward Peninsula, Alaska. *Journal of Geophysical Research*, *112*(F2). https://doi.org/10.1029/2006JF000554

Lindgren, P. R., Farquharson, L. M., Romanovsky, V. E., & Grosse, G. (2021). Landsat-based lake distribution and changes in western Alaska permafrost regions between the 1970s and 2010s. *Environmental Research Letters*, *16*(2), 025006. https://doi.org/10.1088/1748-9326/abd270

Mackay, J. R. (1988). *Catastrophic lake drainage, Tuktoyaktuk Peninsula area, District of Mackenzie*. Geological Survey of Canada. 88-1D.
Marsh, P., & Bigras, S. C. (1988). Evaporation from Mackenzie Delta lakes, N.W.T., Canada. *Arctic and Alpine Research*, *20*(2), 220–229. https://doi.org/10.2307/1551500
Marsh, P., Russell, M., Pohl, S., Haywood, H., & Onclin, C. (2009). Changes in thaw lake drainage in the Western Canadian Arctic from 1950 to 2000. *Hydrological Processes*, *23*(1), 145–158. https://doi.org/10.1002/hyp.7179
McLeod, A. I. (2011). *Kendall: Kendall rank correlation and Mann-Kendall trend test. R package version 2.2*. Retrieved from https://CRAN.R-project.org/package=Kendall
Narita, K., Harada, K., Saito, K., Sawada, Y., Fukuda, M., & Tsuyuzaki, S. (2015). Vegetation and permafrost thaw depth 10 Years after a tundra fire in 2002, Seward Peninsula, Alaska. *Arctic Antarctic and Alpine Research*, *47*(3), 547–559. https://doi.org/10.1657/AAAR0013-031
Nitze, I., Cooley, S., Duguay, C., Jones, B. M., & Grosse, G. (2020). The catastrophic thermokarst lake drainage events of 2018 in northwestern Alaska: Fast-forward into the future. *The Cryosphere Discussions*, 1–33. https://doi.org/10.5194/tc-2020-106
Nitze, I., Grosse, G., Jones, B., Arp, C., Ulrich, M., Fedorov, A., & Veremeeva, A. (2017). Landsat-based trend analysis of lake dynamics across northern permafrost regions. *Remote Sensing*, *9*(7), 640. https://doi.org/10.3390/rs9070640
NWT Centre for Geomatics. (2020). *Fire history: Fire history data of the NWT*. Retrieved from http://www.geomatics.gov.nt.ca/Downloads/Vector/Biota/FireHistory
Olthof, I., Fraser, R. H., & Schmitt, C. (2015). Landsat-based mapping of thermokarst lake dynamics on the Tuktoyaktuk Coastal Plain, Northwest Territories, Canada since 1985. *Remote Sensing of Environment*, *168*, 194–204. https://doi.org/10.1016/j.rse.2015.07.001
O'Neill, H. B., Wolfe, S. A., & Duchesne, C. (2019). New ground ice maps for Canada using a paleogeographic modelling approach. *The Cryosphere*, *13*(3), 753–773. https://doi.org/10.5194/tc-13-753-2019
Pastick, N. J., Jorgenson, M. T., Goetz, S. J., Jones, B. M., Wylie, B. K., Minsley, B. J., et al. (2019). Spatiotemporal remote sensing of ecosystem change and causation across Alaska. *Global Change Biology*, *25*(3), 1171–1189. https://doi.org/10.1111/gcb.14279
Plug, L. J., Walls, C., & Scott, B. M. (2008). Tundra lake changes from 1978 to 2001 on the Tuktoyaktuk Peninsula, western Canadian Arctic. *Geophysical Research Letters*, *35*(3). https://doi.org/10.1029/2007GL032303
Pohl, S., Marsh, P., Onclin, C., & Russell, M. (2009). The summer hydrology of a small upland tundra thaw lake: Implications to lake drainage. *Hydrological Processes*, *23*(17), 2536–2546. https://doi.org/10.1002/hyp.7238
Porter, C., Morin, P., Howat, I., Noh, M. J., Bates, B., Peterman, K., et al. (2018). *ArcticDEM. Harvard Dataverse, V1*. https://doi.org/10.7910/DVN/OHHUKH
R Core Team. (2020). *R: A language and environment for statistical computing*. R Foundation for Statistical Computing. Retrieved from https://www.R-project.org/
Roach, J. K., Griffith, B., & Verbyla, D. (2013). Landscape influences on climate-related lake shrinkage at high latitudes. *Global Change Biology*, *19*(7), 2276–2284. https://doi.org/10.1111/gcb.12196
Rover, J., Ji, L., Wylie, B. K., & Tieszen, L. L. (2012). Establishing water body areal extent trends in interior Alaska from multi-temporal Landsat data. *Remote Sensing Letters*, *3*(7), 595–604. https://doi.org/10.1080/01431161.2011.643507
Schuur, E. a. G., McGuire, A. D., Schädel, C., Grosse, G., Harden, J. W., Hayes, D. J., et al. (2015). Climate change and the permafrost carbon feedback. *Nature*, *520*(7546), 171–179. https://doi.org/10.1038/nature14338
Serreze, M. C., Barrett, A. P., Stroeve, J. C., Kindig, D. N., & Holland, M. M. (2009). The emergence of surface-based Arctic amplification. *The Cryosphere*, *9*. https://doi.org/10.5194/tc-3-11-2009
Smith, L. C., Sheng, Y., MacDonald, G. M., & Hinzman, L. D. (2005). Disappearing Arctic lakes. *Science*, *208*, 14291429. https://doi.org/10.1126/science.1108142
Smol, J. P., & Douglas, M. S. V. (2007). Crossing the final ecological threshold in high Arctic ponds. *Proceedings of the National Academy of Sciences*, *104*(30), 12395–12397. https://doi.org/10.1073/pnas.0702777104
Swanson, D. K. (2019). Thermokarst and precipitation drive changes in the area of lakes and ponds in the National Parks of northwestern Alaska, 1984–2018. *Arctic Antarctic and Alpine Research*, *51*(1), 265–279. https://doi.org/10.1080/15230430.2019.1629222
Turner, K. W., Wolfe, B. B., Edwards, T. W. D., Lantz, T. C., Hall, R. I., & Larocque, G. (2014). Controls on water balance of shallow thermokarst lakes and their relations with catchment characteristics: A multi-year, landscape-scale assessment based on water isotope tracers and remote sensing in Old Crow Flats, Yukon (Canada). *Global Change Biology*, *20*(5), 1585–1603. https://doi.org/10.1111/gcb.12465
Wang, L., Jolivel, M., Marzahn, P., Bernier, M., & Ludwig, R. (2018). Thermokarst pond dynamics in subarctic environment monitoring with radar remote sensing. *Permafrost and Periglacial Processes*, *29*(4), 231–245. https://doi.org/10.1002/ppp.1986
Warnes, G. R., Bolker, B. M., Lumley, T., & Johnson, R. C. (2018). *Gmodels: Various R Programming Tools for model fitting. R package version 2.18.1*. Retrieved from https://CRAN.R-project.org/package=gmodels
Watts, J. D., Kimball, J. S., Jones, L. A., Schroeder, R., & McDonald, K. C. (2012). Satellite microwave remote sensing of contrasting surface water inundation changes within the Arctic–Boreal Region. *Remote Sensing of Environment*, *127*, 223–236. https://doi.org/10.1016/j.rse.2012.09.003
Wickham, H. (2016). *ggplot2: Elegant Graphics for data analysis* (3rd ed.). Springer-Verlag.
Wickham, H., François, R., Henry, L., & Kirill, M. (2020). *Dplyr: A Grammar of data Manipulation. R package version 0.8.5*. https://CRAN.R-project.org/package=dplyr
Wickham, H., & Henry, L. (2020). *Tidyr: Tidy Messy data. R package version 1.0.2*. Retrieved from https://CRAN.R-project.org/package=tidyr
Wood, S. N. (2011). Fast stable restricted maximum likelihood and marginal likelihood estimation of semiparametric generalized linear models. *Journal of the Royal Statistical Society*, *73*(1), 3–36. https://doi.org/10.1111/j.1467-9868.2010.00749.x
Wood, S. N. (2017). *Generalized additive models: An introduction with R* (2nd ed.). Chapman and Hall.
Yoshikawa, K., Bolton, W. R., Romanovsky, V. E., Fukuda, M., & Hinzman, L. D. (2002). Impacts of wildfire on the permafrost in the boreal forests of Interior Alaska. *Journal of Geophysical Research*, *107*(D1). FFR 4-1-FFR 4-14. https://doi.org/10.1029/2001JD000438
Yoshikawa, K., & Hinzman, L. D. (2003). Shrinking thermokarst ponds and groundwater dynamics in discontinuous permafrost near council, Alaska. *Permafrost and Periglacial Processes*, *14*(2), 151–160. https://doi.org/10.1002/ppp.451
Zeileis, A. (2004). Implementing a class of structural change tests: An econometric computing approach. *Computational Statistics & Data Analysis*, *50*, 2987–3008.
Zeileis, A., & Grothendieck, G. (2005). Zoo: S3 infrastructure for regular and irregular time series. *Journal of Statistical Software*, *14*(6), 1–27. https://doi.org/10.18637/jss.v014.i06
Zipper, S. C., Lamontagne-Hallé, P., McKenzie, J. M., & Rocha, A. V. (2018). Groundwater controls on postfire permafrost thaw: Water and energy balance effects. *Journal of Geophysical Research: Earth Surface*, *123*(10), 2677–2694. https://doi.org/10.1029/2018JF004611